Journal of Sound and Vibration (2003) **259**(5), 1253–1264
doi:10.1006/jsvi.2002.5289, available online at http://www.idealibrary.com on IDEAL®

HARMONIC OSCILLATIONS, STABILITY AND CHAOS CONTROL IN A NON-LINEAR ELECTROMECHANICAL SYSTEM

R. Yamapi and J. B. Chabi Orou

Institut de Mathématiques et de Sciences Physiques, B.P. 613*, Porto-Novo, Bénin*
AND
P. Woafo

Laboratoire de Mécanique, Faculté des Sciences, Université de Yaoundé I, B.P. 812*, Yaoundé, Cameroun. E-mail: pwoafo@uycdc.uninet.cm*

(*Received* 2 *January* 2002, *and Accepted* 27 *May* 2002)

1. INTRODUCTION

Coupled oscillators play an important role in different scientific disciplines, ranging from biology, chemistry and physics to engineering. In recent years, considerable effort has been devoted to the study of oscillatory and chaotic states of some non-linear coupled oscillators [1–5]. Among these coupled systems, a particular class is that containing the Duffing oscillator encountered in various electrical systems. Subjected to external sinusoidal excitation, the Duffing oscillator leads to various phenomena: harmonic, subharmonic and superharmonic oscillations, and chaotic behavior [1, 6, 7].

Considering the coupling between two Duffing oscillators or between the Duffing oscillator and other types of oscillators, some interesting results have recently been obtained. Kozlowski *et al.* [8] have analyzed various bifurcations of two coupled periodically driven Duffing oscillators. They showed that the global pattern of bifurcation curves in the parameter space consists of repeated subpatterns similar to the superstructure observed for single, periodically driven, strictly dissipative oscillators.

For the coupling between a Duffing oscillator and self-sustained oscillators, the problem was considered in reference [2] by investigating the dynamics of a system consisting of a Van der Pol oscillator coupled dissipatively and elastically to a Duffing oscillator. Using the multiple time scales method, the oscillatory states were analyzed both in the resonant and non-resonant cases. Chaos was also found using the Shilnikov theorem. This paper considers the behavior of an electromechanical system consisting of a Duffing oscillator coupled to a linear oscillator. The model is interesting since it is widely encountered in electromechanical engineering as described in section 2.1.

Three major problems are considered in the paper. In section 2, the harmonic oscillations and their stability are studied using, respectively, the method of harmonic balance and the Floquet theory. Section 3 analyzes some bifurcation structures and the transitions from regular behavior to chaos. The indicators used are the one-dimensional Lyapunov exponent and the bifurcation diagrams. Finally, the canonical feedback controller algorithm [9] is used to drive the electromechanical transducer from chaos to a regular target trajectory. Section 4 is devoted to the conclusions.

0022-460X/02/$35.00

2. DESCRIPTION OF THE MODEL AND OSCILLATORY STATES

2.1. DESCRIPTION OF THE MODEL

The electromechanical device shown in Figure 1 is an electromechanical transducer. It is composed of an electrical part (Duffing oscillator) coupled to a mechanical part governed by the linear oscillator. The coupling between both parts is realized through the electromagnetic force due to a permanent magnet. It creates a Laplace force in the mechanical part and the Lenz electromotive voltage in the electrical part. The electrical part of the system consists of a resistor R, an inductor L, a condenser C and a sinusoidal voltage source $e(\tau') = v_0 \cos \Omega\tau'$ (v_0 and Ω being, respectively, the amplitude and frequency, and τ' the time), all connected in series. In the present model, the voltage of the condenser is a non-linear function of the instantaneous electrical charge q. It can be written as follows:

$$V_c = \frac{1}{C_0} q + a_3 q^3, \tag{1}$$

where C_0 is the linear value of C and a_3 is a non-linear coefficient depending on the type of the capacitor in use. The mechanical part is composed of a mobile beam which can move along the $\vec{z}$-axis on both sides. The rod T which has the similar motion is bound to a mobile beam with a spring.

Using the electrical and mechanical laws, and taken into account the contributions of the Laplace force and the Lenz electromotive voltage, it is found that the system is described by the following set of differential equations:

$$\begin{aligned} L\ddot{q} + R\dot{q} + \frac{q}{C_0} + a_3 q^3 + lB\dot{z} &= v_0 \cos \Omega\tau', \\ m\ddot{z} + \lambda\ddot{z} + kz - lB\dot{q} &= 0, \end{aligned} \tag{2}$$

where l is the length of the domain of the interaction between $\vec{B}$ and the two mobile rods supporting the beam. The dot over a quantity denotes the time derivative. Now use the

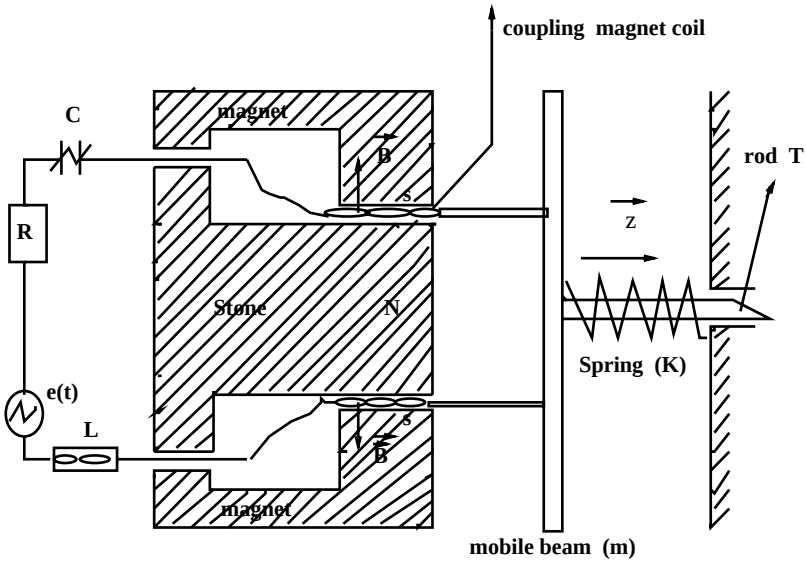

Figure 1. The electromechanical transducer.

dimensionless variables

$$x = \frac{q}{Q_0}, \qquad y = \frac{z}{l}, \qquad t = w_e \tau', \tag{3}$$

where Q_0 is a reference charge of the condenser and

$$\begin{aligned} w_e^2 &= \frac{1}{LC_0}, \quad w_m^2 = \frac{k}{m}, \quad \gamma_1 = \frac{R}{Lw_e}, \\ \beta &= \frac{a_3 Q_0^2}{Lw_e^2}, \quad \lambda_1 = \frac{l^2 B}{LQ_0 w_e}, \quad E_0 = \frac{v_0}{LQ_0 w_e^2}, \\ w &= \frac{\Omega}{w_e}, \quad \gamma_2 = \frac{\lambda}{mw_e}, \quad w_2 = \frac{w_m}{w_e}, \quad \lambda_2 = \frac{BQ_0}{mw_e} \end{aligned} \tag{4}$$

Then the differential equations (2) reduce to the following set of non-dimensional differential equations:

$$\begin{aligned} \ddot{x} + \gamma_1 \dot{x} + x + \beta x^3 + \lambda_1 \dot{y} &= E_0 \cos wt, \\ \ddot{y} + \gamma_2 \dot{y} + w_2^2 y - \lambda_2 \dot{x} &= 0. \end{aligned} \tag{5}$$

The model represented by Figure 1 is widely encountered in various branches of electromechanical engineering. In particular, in its linear version, it describes the well-known electrodynamic loud-speaker [10]. In the case, the sinusoidal signal $e(t)$ represents an incomming pure message. Because of the recent advances in the theory of non-linear phenomena, it is interesting to consider such an electro-dynamic system containing one or various non-linear components or in the state where one or various of its component react non-linearly. One such state occurs in the electrodynamic loudspeaker due to the non-linear character of the diaphragm suspension system resulting in signal distorsion and subharmonics generation [10]. Moreover, the model can serve as servo-command mechanism which can be used for various applications. Here one would like to take advantage of non-linear responses of the model in manufacturing processes.

2.2. FORCED HARMONIC OSCILLATORY STATES

Equations (5) are solved by using the harmonic balance method. For this purpose, express x and y in the form

$$\begin{aligned} x &= a_1 \cos wt + a_2 \sin wt, \\ y &= b_1 \cos wt + b_2 \sin wt. \end{aligned} \tag{6}$$

Set $A^2 = a_1^2 + a_2^2$ and $B^2 = b_1^2 + b_2^2$. Inserting equations (6) into equations (5) and equating the cosine and sine terms separately, one obtains

$$\begin{aligned} \left(1 - w^2 + \tfrac{3}{4}\beta A^2\right) a_1 + \gamma_1 w a_2 + \lambda_1 w b_2 &= E_0, \\ -w\gamma_1 a_1 + \left(1 - w^2 + \tfrac{3}{4}\beta A^2\right) a_2 - \lambda_1 w b_1 &= 0, \\ \left(w_2^2 - w^2\right) b_1 + \gamma_2 w b_2 - \lambda_2 w a_2 &= 0, \\ -w\gamma_2 b_1 + \left(w_2^2 - w^2\right) b_2 + \lambda_2 w a_1 &= 0. \end{aligned} \tag{7}$$

After some algebraic manipulations, one finds that the amplitudes A and B satisfy the following equations:

$$\begin{aligned} \tfrac{9}{16}\beta^2 A^6 + \tfrac{3}{2}\beta F A^4 + \left(F^2 + G^2\right) A^2 - E_0^2 &= 0, \\ B &= \frac{\lambda_2 w}{\sqrt{D}} A, \end{aligned} \tag{8}$$

where

$$D = \left(w_2^2 - w^2\right)^2 + w^2\gamma_2^2,$$
$$F = 1 - w^2 - \frac{\lambda_1\lambda_2 w^2\left(w_2^2 - w^2\right)}{D},$$
$$G = \gamma_1 w + \frac{\lambda_1\lambda_2\gamma_2 w^3}{D}. \tag{9}$$

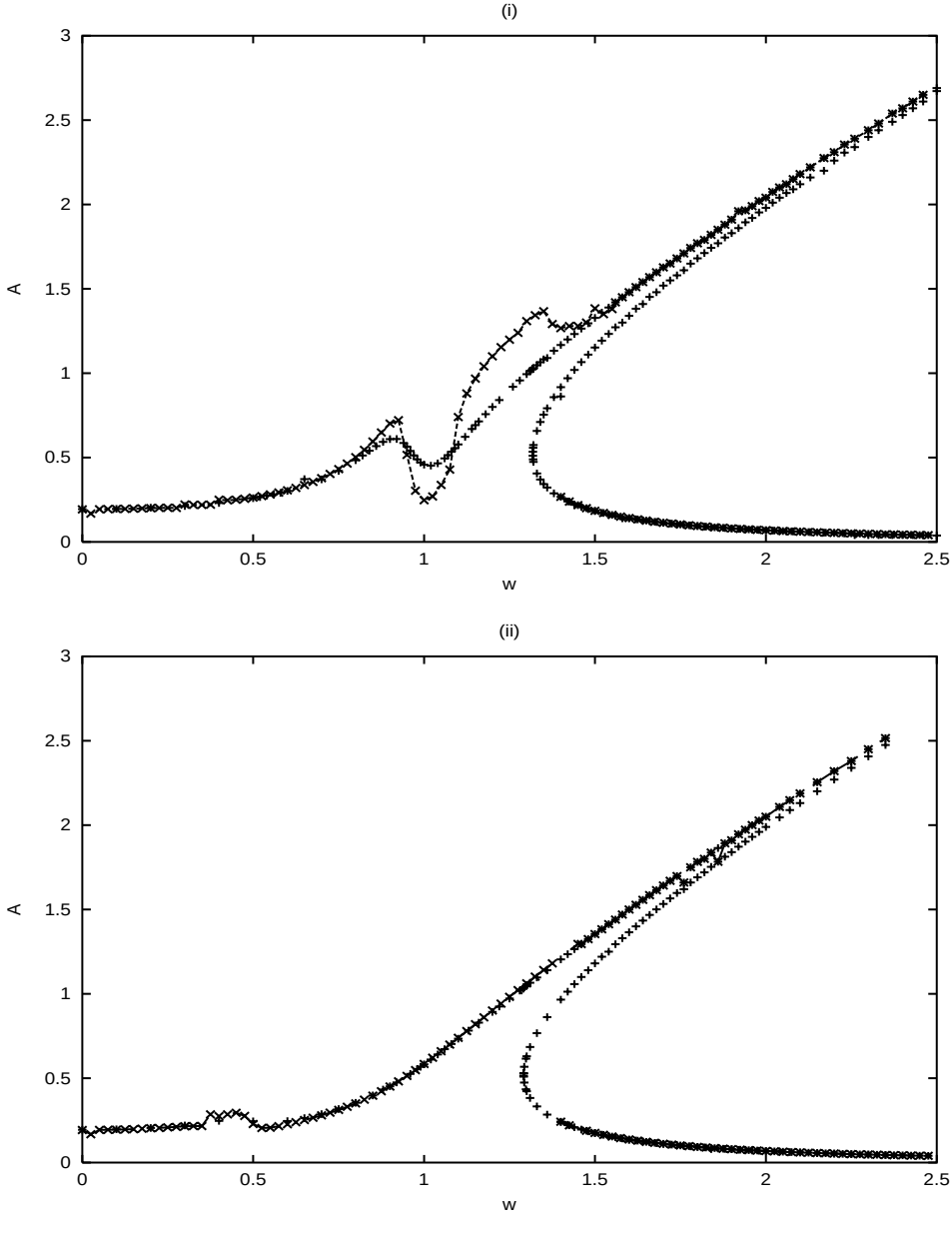

Figure 2. Analytical (+) and numerical (— × —) frequency–response curves $A(w)$, with the parameters $E_0 = 0{\cdot}2$, $\gamma_1 = 0{\cdot}01$, $\gamma_2 = 0{\cdot}1$, $\lambda_1 = 0{\cdot}2$, $\lambda_2 = 0{\cdot}4$, $\beta = 0{\cdot}95$. (i) $w_2 = 1{\cdot}0$, (ii) $w_2 = 0{\cdot}5$.

Using the Newton–Raphson algorithm, one finds A and B when the frequency w is varied. The analytical and numerical frequency–response curves obtained are provided in Figure 2 for A and in Figure 3 for B. The curves show antiresonance and resonance peaks besides the hysteresis domains. Figure 4 shows the amplitude–response curves of the Duffing oscillator for three fixed values of γ_1 in the case of the internal resonance ($w_2 = 1$) and the non-resonant case ($w_2 \neq 1$). The curves show the jump phenomena.

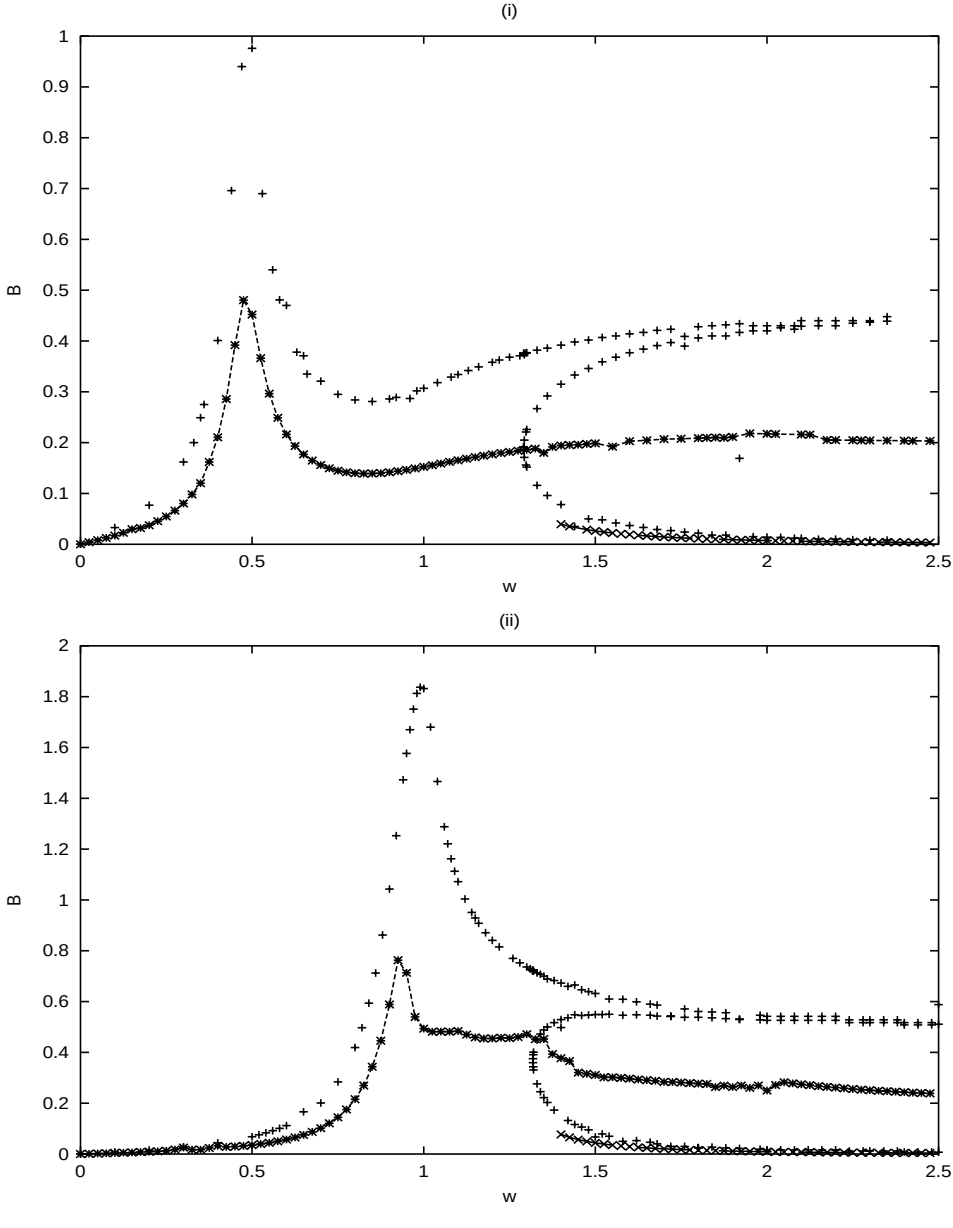

Figure 3. Analytical (+) and numerical (— × —) frequency–response curves $B(w)$. (i) $w_2 = 1{\cdot}0$, (ii) $w_2 = 0{\cdot}5$. The other parameters are those of Figure 2.

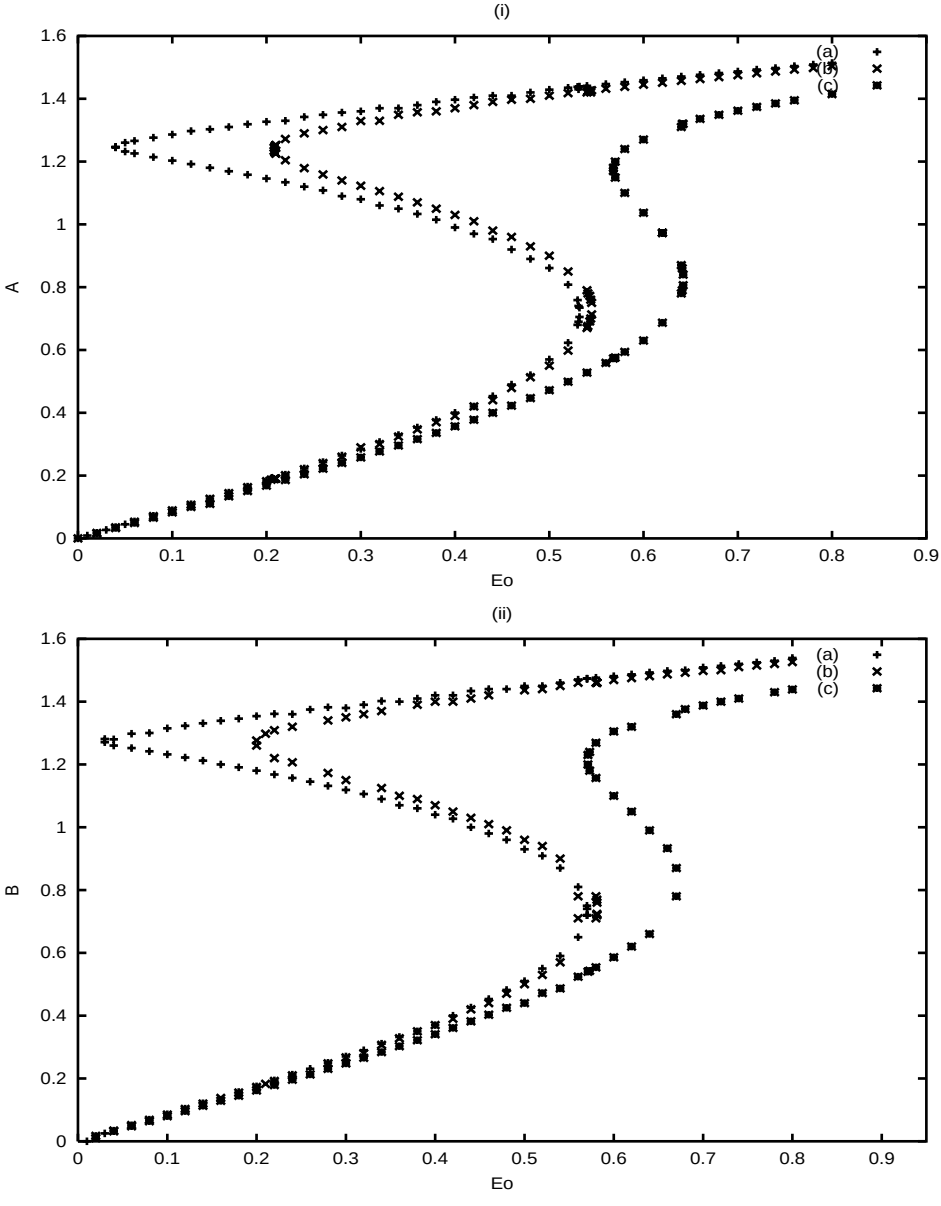

Figure 4. Amplitude–response curves $A(E_0)$. (i) $w_2 = 1{\cdot}0$, (ii) $w_2 = 0{\cdot}5$. The other parameters are those of Figure 2 and $w = 1{\cdot}5$. with (a) $\gamma_1 = 0{\cdot}01$, (b) $\gamma_1 = 0{\cdot}1$, (c) $\gamma_1 = 0{\cdot}3$.

3. STABILITY OF THE HARMONIC OSCILLATIONS

To study the stability of the oscillatory states, consider the following variational equations of equations (5) around the oscillatory states given by equation (6)

$$\begin{aligned} \delta\ddot{x} + \gamma_1\delta\dot{x} + \delta x + 3\beta x_s^2\delta x + \lambda_1\delta\dot{y} = 0, \\ \delta\ddot{y} + \gamma_2\delta\dot{y} + w_2^2\delta y - \lambda_2\delta\dot{x} = 0, \end{aligned} \tag{10}$$

where x_s is the oscillatory state defined by equations (6).

The oscillatory states (x_s, y_s) are stable if δx and δy remain bounded as the time goes up. The appropriate analytical tool to investigate the stability conditions of the oscillatory states is the Floquet theory [1]. Now express δx and δy in the form

$$\begin{aligned} \delta x &= u(t)\exp(-\varepsilon_a \tau), \\ \delta y &= v(t)\exp(-\varepsilon_b \tau), \end{aligned} \tag{11}$$

where $\varepsilon_a = \gamma_1/w$, $\varepsilon_b = \gamma_2/w$, $\varepsilon = \varepsilon_b - \varepsilon_a$, $t = 2\tau/w$.

Inserting equations (11) into equations (10), one obtains

$$\begin{aligned} &\frac{\mathrm{d}^2 u}{\mathrm{d}\tau^2} + [\delta_{11} + 2\varepsilon_{11}\cos(4\tau - 2\phi)]u + \delta_{12}\exp(-\varepsilon\tau)v \\ &+ c_1 \frac{\mathrm{d}v}{\mathrm{d}\tau}\exp(-\varepsilon\tau) = 0, \\ &\frac{\mathrm{d}^2 v}{\mathrm{d}\tau^2} + \delta_{21}\exp(\varepsilon\tau)u + \delta_{22}v + c_2\frac{\mathrm{d}u}{\mathrm{d}\tau}\exp(\varepsilon\tau) = 0, \end{aligned} \tag{12}$$

where the new parameters δ_{ij} and ε_{11} are given by

$$\begin{aligned} \delta_{11} &= -\varepsilon_a^2 + \frac{4}{w^2} + \frac{3\beta A^2}{w^2}, \quad \delta_{12} = \frac{-2\lambda_1\varepsilon_b}{w}, \\ \delta_{22} &= -\varepsilon_b^2 + \frac{2w_2^2}{w^2}, \quad \delta_{21} = \frac{2\varepsilon_a\lambda_2}{w}, \quad \varepsilon_{11} = \frac{3\beta A^2}{2w^2}, \\ c_1 &= \frac{2\lambda_1}{w}, \quad c_2 = \frac{-2\lambda_2}{w}. \end{aligned} \tag{13}$$

Following the Floquet theory [1], the small Hill determinant gives the following equation:

$$\begin{aligned} \Delta(\varepsilon_a, \varepsilon_b) &= [(\delta_{11} + \varepsilon_a^2)(\delta_{22} + \varepsilon_b^2) - (\delta_{12} + c_1\varepsilon_b)(\delta_{21} + c_2\varepsilon_a)] \\ &\times \{-(\delta_{21} + c_2(\varepsilon_a + 2i))(\delta_{12} + c_1(\varepsilon_b - 2i)) \\ &\times \{(\delta_{11} + (\varepsilon_a - 2i)^2)(\delta_{22} + (\varepsilon_b - 2i)^2) - (\delta_{12} + c_1(\varepsilon_b - 2i))(\delta_{21} + c_2(\varepsilon_a - 2i))\} \\ &- (\delta_{22} + (\varepsilon_b + 2i)^2)(\delta_{11} + (\varepsilon_a + 2i)^2)(\delta_{12} + c_1(\varepsilon_b - 2i))(\delta_{21} + c_2(\varepsilon_a + 2i)) + \\ &(\delta_{22} + (\varepsilon_b - 2i)^2)(\delta_{22} + (\varepsilon_b + 2i)^2)\{(\delta_{11} + (\varepsilon_a - 2i)^2)(\delta_{11} + (\varepsilon_a + 2i)^2) - \varepsilon_{11}^2\}\} = 0 \end{aligned} \tag{14}$$

for the stability boundary of the harmonic state defined by equations (6).

From the equation, A^2 can be extracted and then substituted into the equation satisfied by A from the harmonic balance method (see equations (8)). This gives the stability boundary as a function of the parameters of the electromechanical system. Figure 5 shows a stability boundary in the (w, E_0) plane both from the analytical treatment (equation (14)) and for the direct numerical checking of the stability boundary from the differential equations. Good agreement is obtained between the analytical and the numerical results.

4. CHAOS CONTROL

The aim of this section is to use the flexibility of the chaotic regime to direct the system to a chosen target trajectory. Let us use the canonical feedback controllers [9, 11, 12]. But before proceeding to the control, first consider the behavior of the model as the amplitude E_0 of the excitation $e(t)$ varies. As in the case of the hard Duffing equation (13), chaos appears in the model only for large value of E_0. Figure 6 shows a chaotic phase portrait while Figure 7 shows a representative bifurcation diagram and the variation of the corresponding Lyapunov exponent. Both curves are obtained by solving numerically, with

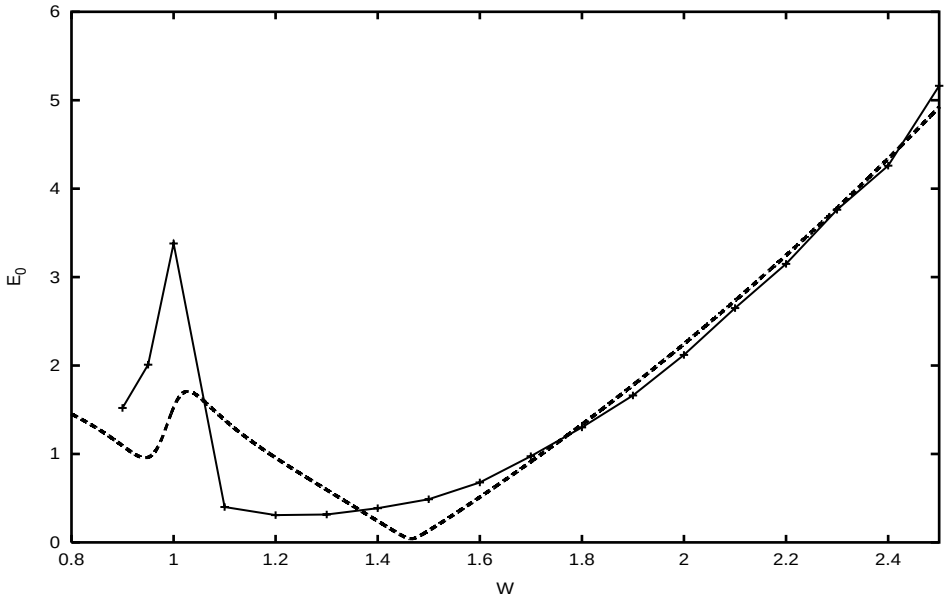

Figure 5. Analytical (- - - -) and numerical (+) stability boundary in the (w, E_0) plane with the parameters of Figure 2.

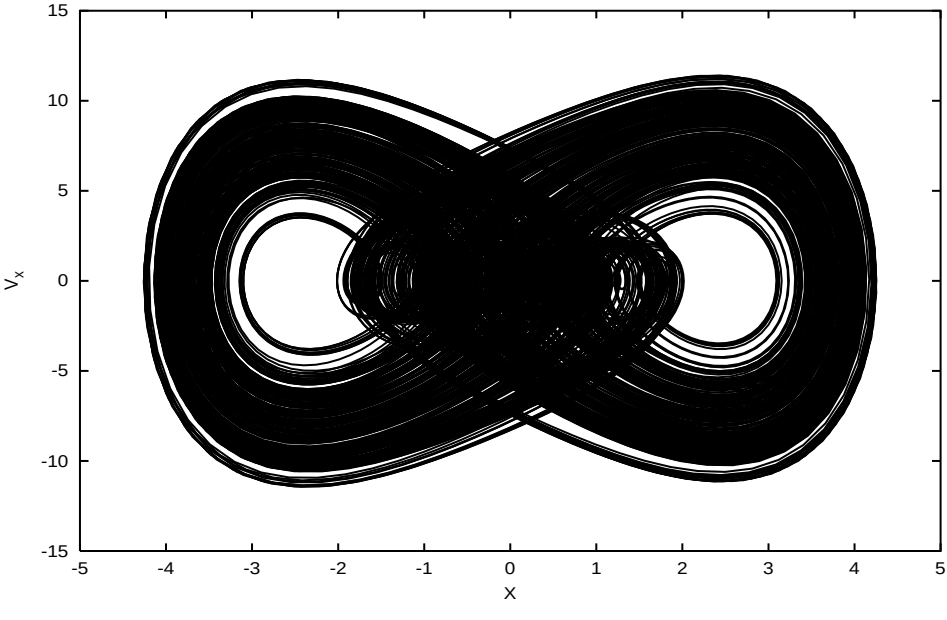

Figure 6. Chaotic phase portrait in the model with the parameters of Figure 7 and $E_0 = 22{\cdot}0$.

the sixth order formulas of the Butcher family of the Runge–Kutta algorithm [14], equation (5) and the corresponding variational equations, the Lyapunov exponent being defined by

$$\mathrm{Lya} = \lim_{t\to\infty} \frac{\ln(\mathrm{d}(t))}{t} \tag{15}$$

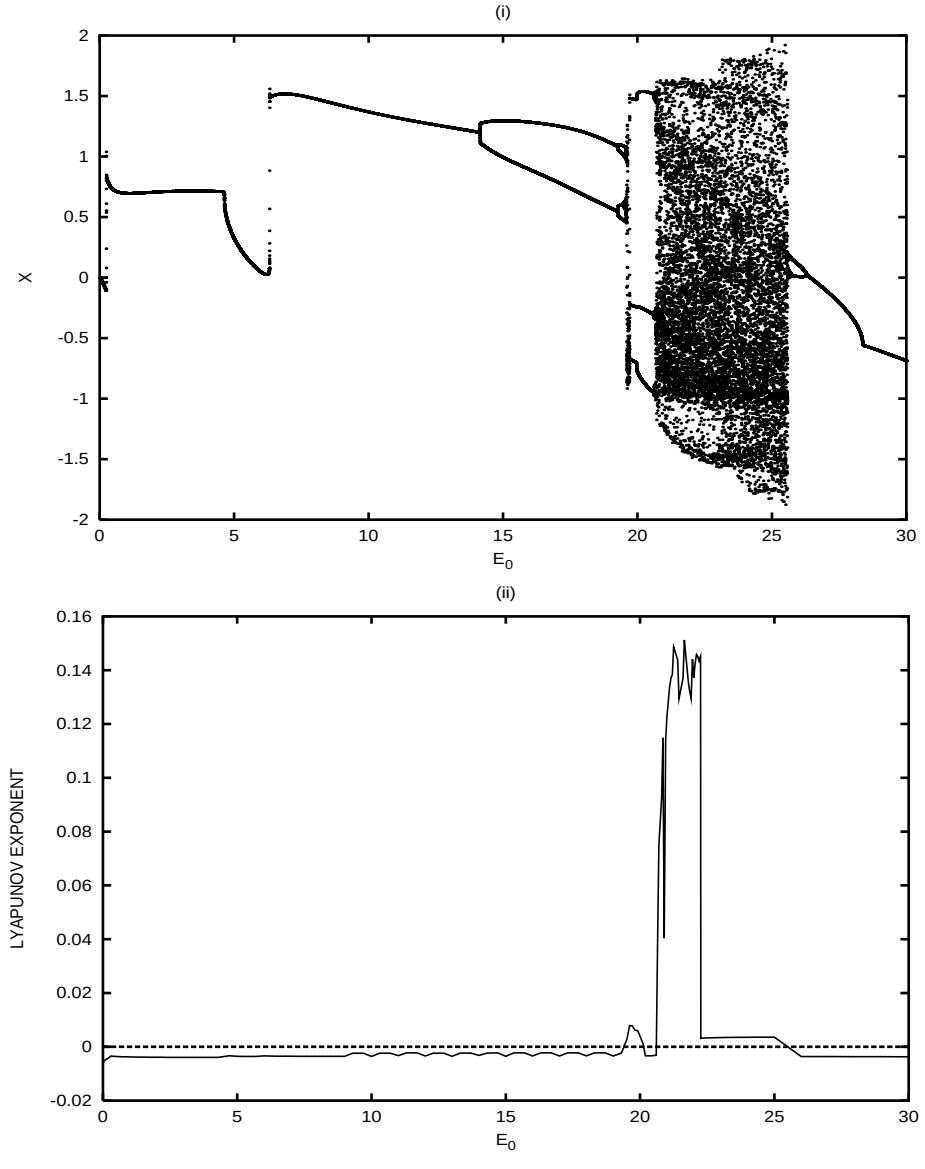

Figure 7. Bifurcation diagram (i) and Lyapunov exponent (ii) when E_0 varies with the parameters $w_2 = 1{\cdot}2$, $w = 1{\cdot}3$, $\gamma_1 = 0{\cdot}1$, $\gamma_2 = 0{\cdot}3$, $\lambda_1 = 0{\cdot}01$; $\lambda_2 = 0{\cdot}06$, $\beta = 1{\cdot}32$.

with

$$\mathrm{d}(t) = \sqrt{\mathrm{d}x^2 + \mathrm{d}v_x^2 + \mathrm{d}y^2 + \mathrm{d}v_y^2}, \tag{16}$$

where $\mathrm{d}x$, $\mathrm{d}v_x$, $\mathrm{d}y$ and $\mathrm{d}v_y$ are the variations of x, $\dot{x}$, y and $\dot{y}$ respectively. As it appears, different types of bifurcations take place before the onset of chaos. As E_0 increases from zero, the amplitude of the symmetrical periodic oscillations increases until $E_0 = 4{\cdot}67$ where the symmetrical behavior bifurcates into an asymmetrical oscillatory state. Then at $E_0 = 6{\cdot}15$, a tiny multiperiodic transition appears and the system passes into another periodic state. As E_0 increases further, a period doubling transition takes place at

$E_0 = 13{\cdot}76$. At $E_0 = 19{\cdot}17$, the period-2 orbit bifurcates to a period-4 orbit and the period doubling cascade continues leading to a small chaotic window. This window suddenly bifurcates into a period-3 orbit. Another set of period doubling sequences leads to a larger chaotic domain for $E_0 = 20{\cdot}65$–25. But note that for $E_0 = 22{\cdot}6$–25, the system shows a weak or transient chaos characterized by a sort of fractal nature of the basin of attraction. In fact, in this domain, it is found that chaos appears only for some initial conditions. This behavior manifests itself in Figure 7 (ii) by small values of the Lyapunov exponent and in Figure 7 (i) by a sudden expansion of the bifurcation diagram. This type of behavior is characteristic of the hard Duffing equation as reported by Pezeshki and Dowell reference [15]. At the other side of the chaotic domain, a reverse period doubling sequence takes place leading to a period-1 orbit (harmonic oscillations).

Due to the presence of chaos in the electromechanical system, one would like to suppress it or take advantage of the flexibility and the various infinite number of different unstable orbits embedded in the chaotic attractor to tune the system to a desired target regular orbit. The rest of this paper is devoted to this task. We follow the procedure of Chen and Dong [9]. This has also been used recently in Reference [16] for chaos control in electrostatic transducers. Introducing the new variables $x_1 = x$, $x_2 = \dot{x}$, $x_3 = y$, $x_4 = \dot{y}$, equations (5) can then be rewritten as

$$\dot{x}_i = g_i(t, x_1, x_2, x_3, x_4). \tag{17}$$

Let $(\bar{x}_1, \bar{x}_2, \bar{x}_3, \bar{x}_4)$ be the periodic orbit that is being targetted, in the sense that for any given $\varepsilon > 0$, there exists a time $T_\varepsilon > 0$ such that

$$|x_i(t) - \bar{x}_i(t)| \leqslant \varepsilon \quad \text{for all } t \geqslant T_\varepsilon. \tag{18}$$

For this purpose, we use the conventional feedback controllers method to convert the system into

$$\dot{x}_i = g_i(t, x_1, x_2, x_3, x_4) - \sum_{j=1}^{4} K_{ij}(x_j - \bar{x}_j), \tag{19}$$

where the K_{ij} are the feedback gain matrix elements. We restrict ourselves to the case where all $K_{ij} = 0$ except, K_{21} and K_{43} which are assumed to be strictly positive. Then equation (19) becomes

$$\begin{aligned} \dot{x}_1 &= x_2, \\ \dot{x}_2 &= -\gamma_1 x_2 - x_1 - \beta x_1^3 - \lambda_1 x_4 - K_{21}(x_1 - \bar{x}_1) + E_0 \cos wt, \\ \dot{x}_3 &= x_4, \\ \dot{x}_4 &= -\gamma_2 x_4 - w_2^2 x_3 + \lambda_2 x_2 - K_{43}(x_3 - \bar{x}_3). \end{aligned} \tag{20}$$

The control should not introduce additional unstability into the system. It is therefore required that all the roots of the characteristic equation derived from the Jacobian of equations (20) have their real part less than zero. Using the Routh–Hurwitz criterium, gives the condition

$$w_2^2 K_{21} + K_{21} K_{43} + w_2^2(1 + 3\beta \bar{x}_{max}^2) + K_{43}(1 + 3\beta \bar{x}_{max}^2) > 0, \tag{21}$$

where $\bar{x}_{max}$ is the amplitude of the targetting orbit of the first oscillator.

In view of applying the control strategy, we consider the system with the parameters of Figure 7 and $E_0 = 22{\cdot}0$. In this state, this system has a chaotic behavior as it appears in the phase portrait of Figure 6. Two sets of target trajectories have been considered. The first one has the same frequency as the external excitation (period-1 targetting orbit) and is

defined as

$$(\bar{x}_1, \bar{x}_2, \bar{x}_3, \bar{x}_4) = (0.08\cos wt, -0.08w\sin wt, 0.08\cos wt, -0.08w\sin wt). \quad (22)$$

The second set defined by

$$(\bar{x}_1, \bar{x}_2, \bar{x}_3, \bar{x}_4) = (0.08\cos w't, -0.08w'\sin w't, 0.08\cos w't, -0.08w'\sin w't) \quad (23)$$

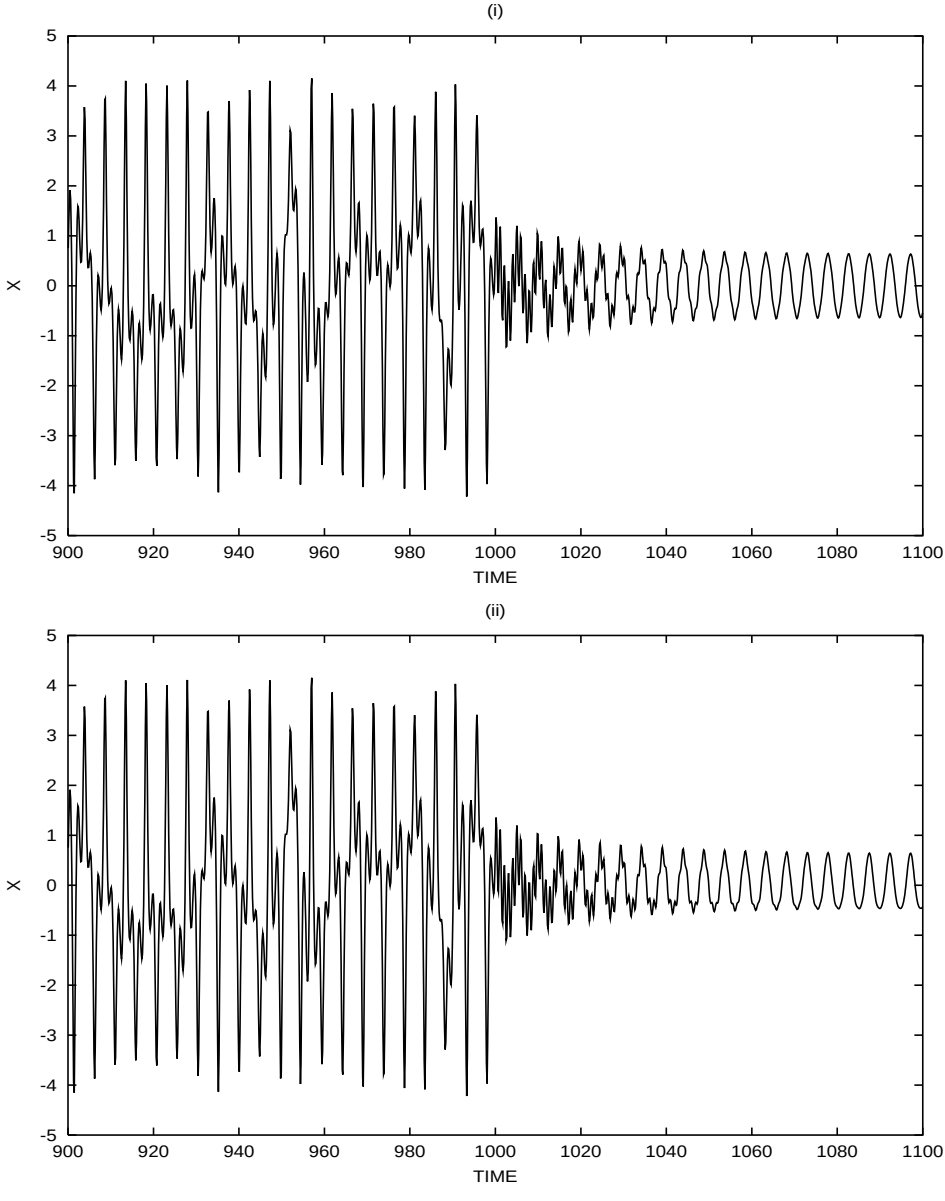

Figure 8. Control to a period-T orbit (i) and to period-$T/2$ orbit (ii) with the parameters of Figure 7.

and has the frequency $w' = 2w$. The feedback matrix elements are $K_{21} = 40$ and $K_{43} = 10$. The results of the control strategy is implemented in Figure 8 and show the efficiency of the control strategy.

5. CONCLUSIONS

In this paper, we have considered the dynamics of an electromechanical system consisting of an electrical Duffing oscillator coupled to a linear mechanical oscillator. The amplitude and the stability boundaries of the harmonic behavior have been obtained using, respectively, the harmonic balance method and the Floquet theory. Bifurcation diagrams showing transitions from regular to chaotic motion have been drawn. The canonical feedback controllers have been used to drive the electromechanical device from a chaotic trajectory to a regular target orbit.

The study has mainly focussed on the harmonic oscillations. We think that an extension of the analytic treatment to find sub- and superharmonic oscillations is an interesting task which can be tackled using the multiple time scales method. Indeed, analyzing and deriving the stability boundaries of each type of oscillations is interesting for the technological exploitation of the devices. Moreover, the behavior of the electromechanical system in the case of parameteric coupling is under consideration. The study of the device with a self-sustained electrical component of the Van der Pol type in place of the Duffing oscillator has been carried out recently [17].

REFERENCES

1. A. H. Nayfeh and D. T. Mook 1979 *Nonlinear Oscillations*. New York: Wiley-Interscience.
2. P. Woafo, J. C. Chedjou and H. B. Fotsin 1996 *Physical Review E* **54**, 5929–5934. Dynamics of a system consisting a Van Der Pol oscillator coupled to a Duffing oscillator.
3. P. Woafo, H. B. Fotsin and J. C. Chedjou 1998 *Physica Scripta* **57**, 195–200. Dynamics of two nonlinearly coupled oscillators.
4. K. R. Asfar and K. K. Masoud 1994 *International Journal of Non-linear Mechanics* **29**, 421–428. Damping of parameterically excited single degree of freedom systems.
5. K. R. Asfar 1989 *Journal of Vibrations, Acoustics, Stress and Reliability in Design* **111**, 130–133. Quenching of self-excited vibrations.
6. C. Hayashi 1964 *Nonlinear Oscillations in Physical Systems*, New York: McGraw-Hill.
7. J. M. Thompson and H. B. Stewart 1986 *Nonlinear Dynamics and Chaos*. New York: John Wiley and Sons.
8. J. Kozlowski, U. Parlitz and W. Lauterborn 1995 *Physical Reivew E* **51**, 1861–1867. Bifurcation analysis of two coupled periodically driven Duffing oscillators.
9. G. Chen and X. Dong 1993 *IEEE Transactions on Circuits and Systems—I: Fundamental Theory and Applications* **40**, 591–601. On feedback control of chaotic continnuos-time systems.
10. H. F. Olson 1967 *Acoustical Engineering*. Princeton, NJ: Van Nostrand.
11. T. Kapitaniak 1996 *Controlling Chaos*. London: Academic Press.
12. M. Lakshmanan and K. Murali 1996 *Chaos in Nonlinear Oscillators, Controlling and Synchronization*. Singapore: World Scientific.
13. U. Parlitz and W. Lauterborn 1985 *Physics Letters A* **107**, 351–355. Superstructure in the bifurcation of the Duffing equation.
14. L. Lapidus and J. H. Seinfeld 1971 *Numerical Solution of Ordinary Differential Equations*. New York, London: Academic Press.
15. C. Pezeshki and E. H. Dowell 1988 *Physica D* **32**, 194–209. On chaos and fractal behavior in a generalized Duffing system.
16. Y. Chembo Kouomou and P. Woafo 2000 *Physica Scripta* **62**, 255–260. Stability and chaos control in electrostatic transducers.
17. J. C. Chedjou, P. Woafo and S. Domngang 2001 *Journal of Vibration and Acoustics* **123**, 170–174. Shilnikov chaos and dynamics of a self-sustained electromechanical transducer.